Proceedings of the Korean Nuclear Society Spring Meeting
Kwangju, Korea, May 1997

Second order VOF convection model in curvilinear coordinates

Seong-O. Kim, Young-dong. Hwang, Young-In. Kim, Moon-Hee. Chang
Korea Atomic Energy Research Institute
P.O. Box 105, Yuseong, Taejeon, Korea, 305-600

ABSTRACT

An approximation technique was developed for the simulation of free surface flows in non-orthogonal coordinates. The main idea of this approach is to approximate VOF by the second order linear equation in the transformed domain on the assumption that the continuity of free surface would be maintained. The method was justified through a set of numerical test to examine if its original shape could be maintained when the circles are convected in uniform velocity in horizontal direction in curvilinear coordinates. Finally a simple problem was solved by applying the method to CFX4.1 general purpose CFDS code.

I. Introduction

There are varieties of physical hydrodynamic phenomena which involve interfaces between phases in nuclear power plant. However, numerical description of phase interfaces is notoriously complicated since the locations of these interfaces are not known in advance and must be determined as part of the solutions of the transport equations.

Reviewing the techniques for dealing with free a surface problem, two kinds of approaches are used. The first one is Lagrangian approach which usually traces particles in Lagrangian method by use of local Eulerian velocities. The approach is applied by boundary integral technique[1-3], finite-element methods[4-6] and boundary-fitted coordinates method[7-9] where every node points on the free surface are moved along the motion of free surface. Therefore the method is hard to apply to the complex situations such as surface folding and surface merging because when two sides of free surface are merged, the merged parts of node point are rearranged to maintain mass continuity.

On the other hand, a numerical technique called the volume tracking metho has the potential for handling large surface deformations and surface folding and merging. This method uses a volumetric progress variable VOF(=Volume of Fraction) but the method developed until now tends to smooth the shapes of interface.[10-13]

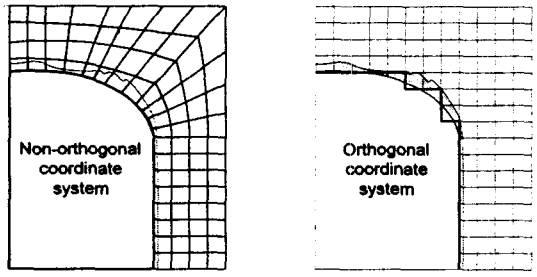

Figure 1. Typical examples of mesh for free surface calculation in orthogonal and non-orthogonal coordinate system

In addition, most of VOF methods are applied to orthogonal coordinates. However, when the methods are applied to a shape of irregular geometry with thin free surface movements, two kinds of problem are expected. The one is to apply boundary condition on the surface of irregular geometry and the other is to control the flow

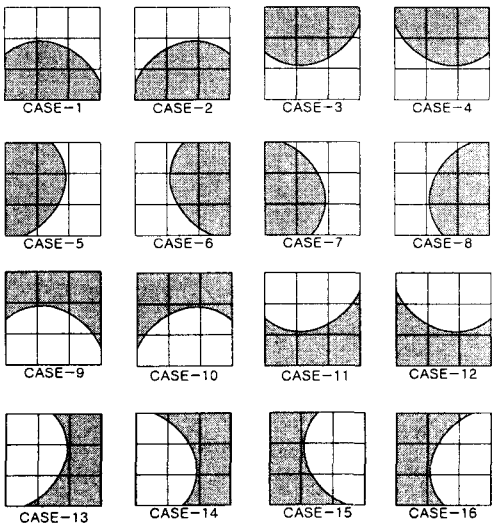

Figure 2 Possible distribution of volume fraction in a cell block

to be contacted on the edged shape of irregular geometry as an example as shown in Figure 1. Therefore, to solve the problem discussed above, a second-order approximation technique will be developed in this study which can be applied to nonorthonal coordinates.

II. Second order model in non-orthogona coordinates

The main idea of this approach comes from the assumption that if the shapes of free surface are continuous in the original domain, the continuity of the shape would be maintained on the transformed domain. Moreover the free surface would be represented with a second order linear equation to prevent from losing curvatures. The procedures of constructing the second-order model for the interfaces and calculating the convective flux are as follows:

Step-1: Define the cell block with 9 cells including the surface cell and its neighboring ones by inspecting the direction of a face velocity,.

Step-2: Calculate slopes of volume fraction, m_R,m_L,m_B and m_T, at every cell faces.

Step-3: Define a second-order linear equation and identify the base cases of the second-order model.

Step-4: Identify the direction of convection and calculate the convective flux.

II.1 Rearrangement of surface cell block

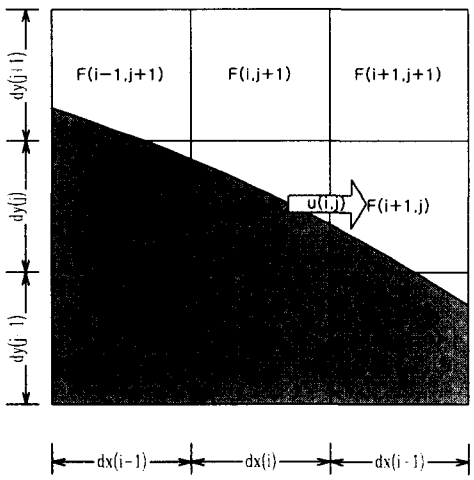

Figure. 3 Typical cell block for case-1

The accuracy of distribution function is very much sensitive to the slope of the face. Also the shape function accuracy impacts convective flux calculation. To enhance the accuracy of the slope calculation, a cell block including the surface cell and environment 8 cells is used. If the face slope is determined only by two adjacent cells, there exist a possibility of losing accuracies when adjacent cells are empty.

When an arbitrary surface cell block is selected from the typical interface, there are varieties of free surface shapes around the surface cell as shown in Figure 2. To reduce the number of cases, the neighboring cell must be rearranged by rotation, trnasition of environmental cells such that the sum of

volume fractions of the bottom row has maximum value and that of the left column has larger value than the right one. By use of this procedure, all the cases are reduced to case-1..

II.2 Slope calculation

After rearranging the surface cell and neighboring cells in the cell block, left face slope is calculated by left two cell columns and right ones are calculated by the right 2 ones. For calculation of the slope at the face of a surface cell, it is assumed that the interface of free surface can be represented either as a single-valued function, f(x) or f(y), for the x,y directions of the model coordinates. Boundary slope 'm' is calculated from the equations (2)-(5) by categorizing the cases based on the value of F_L, F_R, x_L, x_R as shown in Figure 3.

$$f_i = \frac{\sum_{k=j-1}^{j+1} (dy_k F_{i,k})}{H}, \quad \text{where } H = \sum_{k=j-1}^{j+1} dy_k \quad W = dx_i \tag{1}$$

case-1:
$$m = \frac{2}{x_L^2}\left[-(2x_R F_R + x_L F_L) + 2\sqrt{x_R F_L (x_R F_L + x_L F_L)}\right], \tag{2}$$

$$\text{if } F_L \geq \frac{x_R F_L}{2x_R + x_L} \text{ and } x_L(1-F_L) + \sqrt{(F_R(1-F_L)x_L x_R)} \geq \frac{x_L}{2},$$

case-2:
$$m = \frac{2(F_R - F_L)}{(x_R + x_L)}, \tag{3}$$

$$\text{if } F_R \geq \frac{x_R F_L}{2x_R + x_L}, \text{ and } F_R \geq \frac{[F_L(x_R + 2x_L) - (x_R + x_L)]}{x_L},$$

case-3:
$$m = -\frac{1}{2[F_R x_R + \sqrt{F_R(1-F_L)x_R x_L}] + 2[(1-F_L)x_L + \sqrt{F_R(1-F_L)x_R x_L}\ ]}, \tag{4}$$

$$\text{if } x_L(1-F_L) + \sqrt{(F_R(1-F_L)x_L x_R)} \leq \frac{x_L}{2} \text{ and } x_R F_R + \sqrt{F_R(1-F_L)x_R x_L} \leq \frac{x_R}{2},$$

Case-4:
$$m = \frac{-2}{x_R^2}\left[2x_L(1-F_L) + x_R(1-F_R) + 2\sqrt{x_L(1-F_L)\{(x_L(1-F_L) + x_R(1-F_R)\}}\ \right], \tag{5}$$

$$\text{if } F_R \leq \frac{[F_L(x_R + 2x_L) - (x_R + x_L)]}{x_L} \text{ and } x_R F_R + \sqrt{F_R(1-F_L)x_R x_L} \geq \frac{x_R}{2}.$$

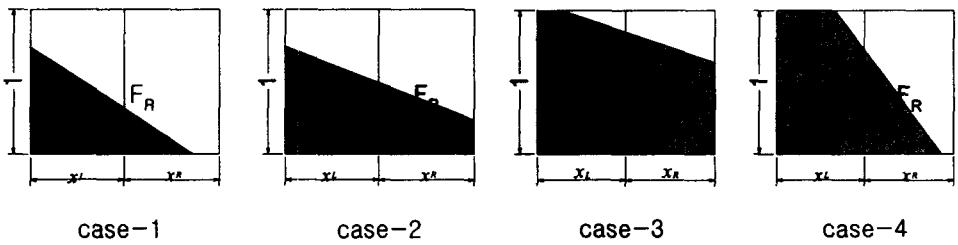

Figure 4 Base case for slope calculation

II.3 Model case identification of surface cell

A second-order linear equation is defined as equation (6) to represent the volume fraction

distribution in a surface cell. The constants a, b are obtained by differentiating the equation and equating it with the slopes at the left and right faces of a surface cell by the equations (7):

$$y = a\xi^2 + b\xi + c \tag{6}$$

$$a = \frac{m_r - m_l}{2} \quad \text{and} \quad b = m_l, \tag{7}$$

where $m_r = dy_j/dx_i \cdot m_R'$, $m_r = dy_j/dx_i \cdot m_L'$ and m_R', m_L' are slope calculated in ξ, η coordinates.

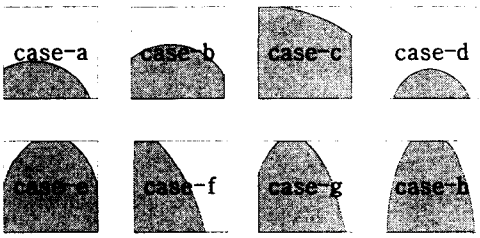

Figure 5. Possible shapes of the interface in a cell when approximating the free surface by the second-order model

When fitting the interfaces of a surface cell by the second-order curve, 8 possible shapes arise as shown Figure 5. However, cases-f, g, h can be excluded by restricting the maximum difference of volume fraction distribution to be less than the cell height. In addition, cases-f, g, h rarely appear if mesh size is small enough and also in these cases, higher than 4th order algebraic equations need to be solved to get the constant 'c' of equation (6).

From the above procedure, the second-order model is categorized into 5-cases(cases-a, b, c, d, e). To calculate the constant 'c' and convective flux, each case is examined by the criteria as described in equations(8)-(13).

$$\text{Case-a} \quad \text{if} \quad F \geq \frac{m_l^3}{(m_l - m_r)^3} \quad \text{and} \quad F \leq -\frac{(2m_r + m_l)}{6}, \tag{8}$$

$$\text{Case-b} \quad \text{if} \quad F \geq -\frac{(2m_r + m_l)}{6} \quad \text{and} \quad F \leq 1 - \frac{(m_l^3 - m_r^3)}{(m_l - m_r)^2}, \tag{9}$$

$$\text{Case-c} \quad \text{if} \quad F \geq 1 + \frac{(m_r + 2m_l)}{6} \quad \text{for} \quad m_l \cdot m_r \geq 0, \tag{10}$$

$$\text{if} \quad F \geq 1 + \frac{m_r - 2m_l}{6}\left(\frac{m_r - m_l}{m_r + m_l}\right)^2 \quad \text{for} \quad m_r \cdot m_l \leq 0, \tag{11}$$

$$\text{case-d} \quad \text{if} \quad F \leq \frac{m_l^3}{6(m_r - m_l)^3}, \tag{12}$$

$$\text{case-e} \quad \text{if} \quad F \geq 1 - \frac{(m_l^3 - m_r^3)}{(m_l - m_r)^2} \quad \text{and} \quad F \leq 1 + \frac{m_r - 2m_l}{6}\left(\frac{m_r - m_l}{m_r + m_l}\right)^2. \tag{13}$$

II.4 Calculation of convective flux

For calculation of convective flux, the direction of convection in the calculation model must be identified since the cell-block is rearranged to reduce the number of cases. To calculate the convective flux, the constant 'c' of equation(7) must be determined. For cases-b, d the constant 'c' determined explicitly from the equation (14),

$$\text{for case-b,} \quad c = F - \frac{2m_r + m_l}{6},$$

$$\text{for case-d,} \quad c = \frac{b^2}{4a} - \frac{a}{4}\left(-\frac{6F}{a}\right)^{2/3}. \tag{14}$$

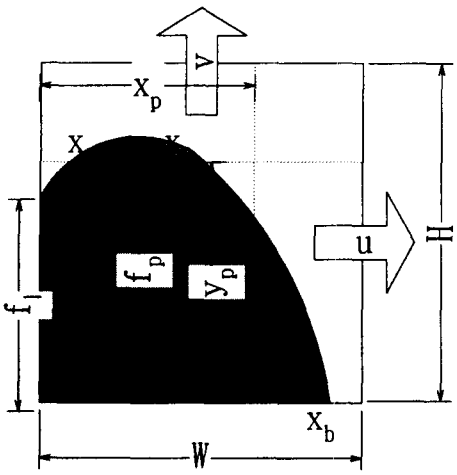

Figure 6. Calculation of convective flux of second order method

For cases-a, c, e the constant 'c' must be evaluated from the third order algebraic equation which comes from integrating the second-order linear equation within the surface cell. After establishing the third-order algebraic equation, an appropriate solution is obtained by the Cardano's solution procedure[14]. For case c and e, the constant 'c' can be obtained by a similar procedure to case-a.

The convective flux in the second-order model is calculated via integration of the second-order equation from the cell face to the distance defined by the local velocity of the cell face over time. For example, for case-a, the flux of volume fraction in the positive x direction is

$$\delta fx=0, \quad \text{if } x_p \geq x_b, \tag{15}$$

$$\delta fx=\int_{x_p}^{x_b} f dx, \text{if } x_p \leq x_b, \text{where } x_p=1-\frac{u \cdot dt}{W}. \tag{16}$$

The flux of the other direction could be calculated in a similar way.

III. Results and Discussion

For testing of convection capability, various sizes of circle are convected from left to the right. The calculation domain was devided in three parts. Left and right hand parts are meshed to have equal length in orthogonal coordinates but center part are meshed by a non-orthogonal coordinate method to check the degree of distortion of a circle during convection process. The non-orthogonal meshes are generated by two methods. At first ξ-direction is generated to be parallel to the x-axis and η-direction mesh is generated by a sine curve(Type-I). At second the ξ-direction one is generated by sine curve and the η-direction one is generated to be parallel to the y-axis(Type-II).

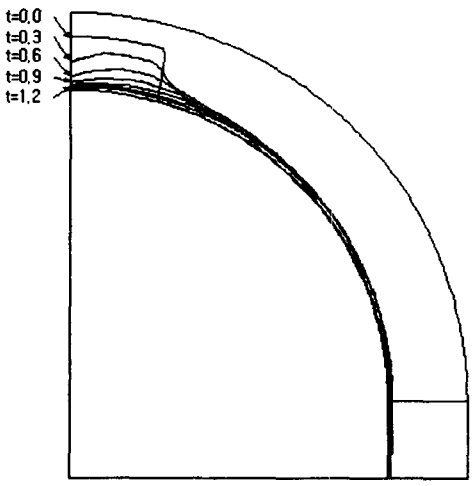

Figure 7. Water column break down simulation by use of CFX 4.1 code with second order free surface convection model

Based on this meshing scheme, each circle is convected from left part to the right part through the non-orthogonal meshes by the 400 time step. The velocities were assigned to have a uniform value (u^i=0.1, v^j=0.0 times of the mesh length of the uniform grid in

convection direction). From the x,y component velocity, contravariant velocities are calculated by the equation (17).

$$u^{\xi} = \frac{u^{x} y_{\eta} - v^{y} x_{\eta}}{\sqrt{g}}, \quad v^{\eta} = \frac{-u^{i} y_{\xi} + v^{j} x_{\xi}}{\sqrt{g}} \tag{17}$$

Similar calculations were conducted by using a first order model developed as FLAIR method[13]. After 400 time step convection, all circles are reconstructed as shown Figure 8,9. To assess the degree of distortion of convected circle, maximum cell error and root of square sum of every cell error v.s. cell diameter are plotted as shown Figure 10-13. The maximum cell error is defined by maximum value of every cell errors normalized by circle area as an indicator of local distortion. The root of square sum error is defined by root of square sum of every cell errors normalized by circle area as an indicator of global distortion of the circles.

From the calculation results, the first and the second order model works well for the non-orthogonal coordinates. However, the first order model has tendencies of being flattened even though the number of cells are increased for circle diameter. The second order model has small distortion for the small diameter(4 cell for diameter) but if the number of cells are increased a little bit, the circle reconstructed by the second order model is completely identical to the exact solution. This result seems to come from the fact that if a circle diameter increase to an extent, second-order model fits the circle completely but the first order model does not fit the curvature of circles exactly even if the number cells are increased. Finally as an example problem, broken dam problem with curvatures base mat was solved for demonstration of second order model to CFX4.1 code as shown Figure 7.

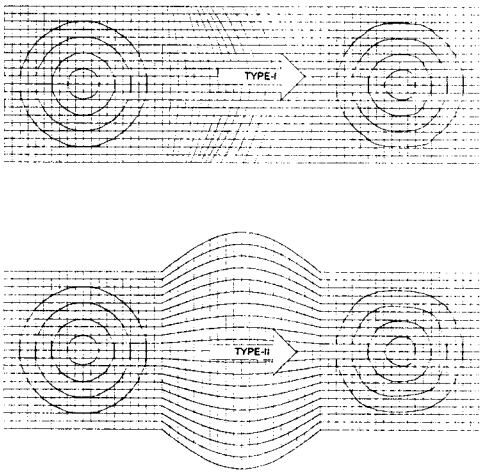

Figure 8. Various sizes of circular geometry after 400 time step convection from left to right hand direction by first order convection method. The radius of circle are 2,4,6,8 times of regular mesh.

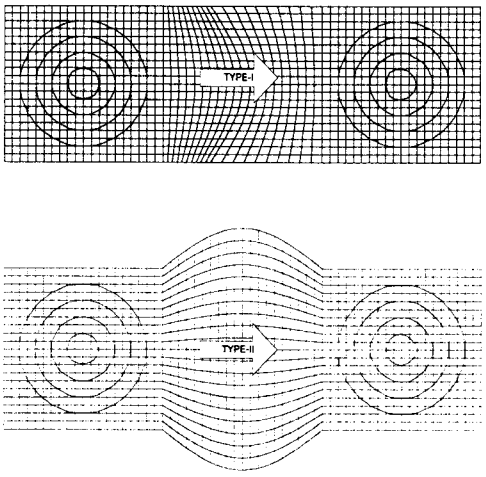

Figure 9. Various sizes of circular geometry after 400 time step convection from left to right hand direction by second order convection method. The radius of circle are 2,4,6,8 times of regular mesh.

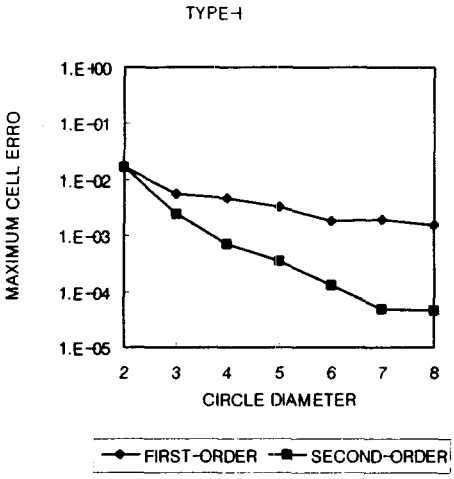

Figure 10. Maximum cell error for the first order and the second order model for the type-1 geometry

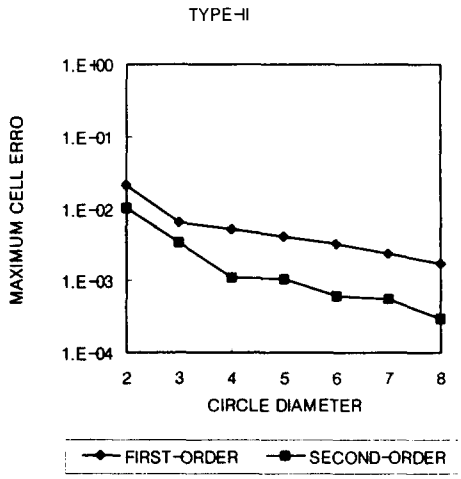

Figure 11. Maximum cell error for the first order and the second order model for the type-2 geometry

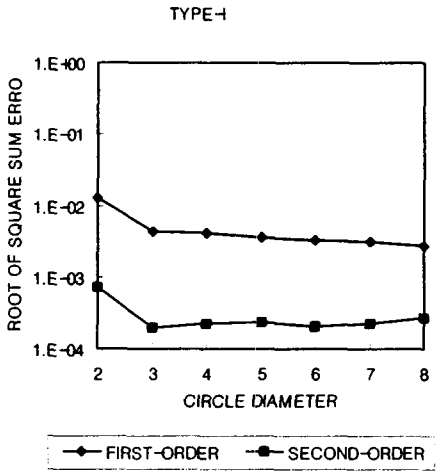

Figure 12. Root of square sum error for the first order and the second order model for the type-1 geometry

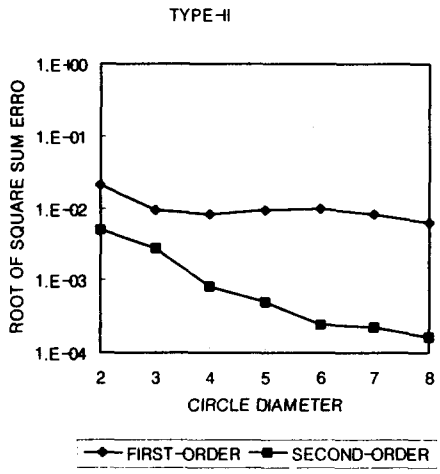

Figure 13. Root of square sum error for the first model and the second order model for the type-2 geometry

IV. Conclusion

An approximation technique was developed for the simulation of free surface flows in non-orthogonal coordinates. The main idea of this approach is to approximate VOF by the second order linear equation on the assumption that the continuity of free surface would be maintained in the transformed domain. To justify the method, A set of numerical test was conducted to examine if its original shape could be maintained. From the test results, it is known that a free surface convection model developed for orthogonal coordinates can be easily

applied to non-orthogonal coordinates through the procedure developed in this study. Moreover the second order method developed in this study shows excellent convection capability of free surface convection. Therefore, for the problem with large curvature of free surface, the second order free surface convection is recommended.

References

1. J.F.Milthorpe and R.I.Tanner, 'Boundary element method for free surface viscous flows', 7th Australian Hydraulics and Fluid Mechanics Conference, Brisbane, 18-22 August (1980).
2. Makoto Natori and Hideo Kawarada, 'Numerical Solution of Free Surface Drainage Problem of Two Immiscible Fluids by the Boundary Element Method', Japanese Journal of Applied Physics, Vol24. 24,No.10,October,1359-1362 (1985).
3. H.C.Henderson, M.Kok and W.L.DE Koning, 'Computer-aided spillway design using the boundary element method and non-linear programming', Int. J. of Numer. Methods in Fluids, Vol,13,625-641(1991).
4. R.Bonnerot and P.Jamet, 'Numerical computation of the free boundary for the problem by space-time elements', J. of Compt. Phys. 25, 163-181 (1977).
5. D.R.Lynch, 'Unified approach to simulation on deforming elements with application to phase change problems' J. of Comput. Phys. 47, 387-411 (1982).
6. P.Bach and O.Hassager, 'An algorithm for the use of the Lagrangian specification in Newtonian fluid mechanics and applications to free-surface flow' J. of Fluid Mech. 152, 173-190 (1985).
7. I.S.Kang and L.G.Leal, 'Numerical solution of axisymmetric, unsteady free-boundary problems at finite Reynolds number. I. Finite-difference scheme and its application to the deformation of a bubble in a uniaxial straining flow' Phys. Fluids 30(7), 1929-1940 (1987).
8. G.Ryskin and L.G.Leal, 'Numerical solution of free-boundary problems in fluid mechanics. Part1. the finite-difference technique', J. of Fluid Mech. 148, 1-17 (1984).
9. N.S.Asaithambi, 'Computation of free-surface flows', J. of Comput. Phys. 73, 380-394 (1987).
10. A.J.Chorin, 'Flame advection and propagation algorithm' J .of Comput. Phys. 35, 1-11 (1980).
11. A.J.Chorin, 'Curvature and solidification' J. of Comput. Phys. 57, 472-490 (1985).
12. D.L.Youngs, Numerical methods for Fluid Dynamics, edited by K.W.Morton and M.J.Baines, Academic Press, New York, (1982).
13. N.Ashgriz and J.Y.Poo, 'FLAIR (Flux Line-Segment Model for Advection and Interface Reconstruction' J. of Comput. Phys. 93, 449-468 (1991).
14. Murray R. Spiegel, Mathematical handbook of formulas and tables in Schaum's outline series, 1968